Rattan, K.J.; Bowes, M.J.; Yates, A.G.; Culp, J.M.; Chambers, P.A. 2021.
Evaluating diffuse and point source phosphorus inputs to streams in a cold climate region using a load apportionment model.

The definitive version was published in *Journal of Great Lakes Research* 47 (3): 761-772. https://doi.org/10.1016/j.jglr.2020.05.003.

The definitive version is available at https://www.elsevier.com/

Evaluating diffuse and point source phosphorus inputs to streams in a cold climate region using a Load Apportionment Model

K. J. Rattan,[a],[*]. M. J. Bowes[b] , A. G. Yates[c], J. M. Culp[d], and P. A. Chambers[a]

[a] K.J. Rattan and P.A. Chambers, Environment and Climate Change Canada, 867 Lakeshore Rd., Burlington, Ontario, L7S 1A1 Canada;

[b] M.J. Bowes, Centre for Ecology and Hydrology, Wallingford Oxon, OX10 8BB, U.K.;

[c] A.G. Yates, Department of Geography, Western University, London Ontario, N6A 3K7, Canada;

[d] J.M. Culp, Wilfrid Laurier University, Faculty of Science, Biology, 75 University Ave West, Waterloo, ON N2L 3C5

[*]Corresponding author. Email address: kjrattan@live.com

Abstract

Variation in the timing and quantity of diffuse versus point-source inputs of phosphorus (P) to streams can be evaluated by assessing P concentration-flow relationships. Diffuse load inputs usually increase with stream flow (due to increased delivery caused by precipitation), whereas point source concentrations decrease with rising river flow (due to increased dilution). This study tested the suitability of a load apportionment model (LAM), a power-law function of flow, to estimate contributions of diffuse and point inputs to P loads for eight sub-watersheds in the Red River Valley, a cold-climate rural region of Manitoba, Canada. For all but two sub-watersheds, annual and seasonal (snowmelt and summer) models of P concentration versus flow best fit a strictly diffuse source contribution. The models identified significant point source inputs (in addition to diffuse sources) to two sub-watersheds, during summer to both watersheds (consistent with the fact that wastewater from sewage lagoons is discharged to upstream reaches between June and September) and during snowmelt for one watershed. Application of a LAM proved to be a simple and rapid method for nutrient source apportionment, detection of unknown sources, for cold-climate rural sub-watersheds. Such information is critical for identifying P sources and, in turn, developing the most effective mitigation strategies to reduce P concentrations and eutrophication risk.

Keywords: Nutrient sources, Eutrophication, Lake Winnipeg, concentration-flow relationships

Introduction

Tributaries play a key role in the biogeochemical connectivity between terrestrial and aquatic ecosystems by controlling the routing and delivery of nutrients such as phosphorus (P) to downstream waterbodies. Knowledge of the timing of P release (seasonal or episodic versus year-round), mode of P delivery (point versus non-point) and within-river transformations of P (through interactions with sediments and river biota) is critical for predicting the magnitude of nutrient export and, in turn, the water quality (eutrophication, algal blooms, species richness) of downstream lakes (Sharpley et al., 1994, Edwards and Withers, 2007). However, identifying the timing of P release and its mode of delivery can be challenging, especially for rural landscapes, and can lead to management inaction when the sources of P cannot be identified or distinguished.

Targeting nutrient sources that will produce the greatest and most cost-effective improvement to water quality requires an understanding of the relative contributions of P inputs to streams. One approach used for source attribution of riverine nutrient loads is the export coefficient method. The method uses coefficients (derived from previous studies) to estimate nutrient loads associated with various land cover types, livestock excretion and wastewater treatment (WWT) plant inputs (Johnes and Heathwaite, 1997, Bowes et al., 2005a, Palviainen et al., 2016). Whilst the method is relatively simple to apply and allows comparison of the relative contributions from diffuse and point sources, major drawbacks are the need for previously-derived coefficients relevant to the study catchment as well as current detailed data on land cover, livestock types and numbers, and population served by WWT plants. Although this approach has been used to assess source contributions to annual nutrient loads (Bowes et al. 2008), it cannot adequately infer seasonal sources of nutrient delivery (Burt and Johnes, 1997). This is a serious disadvantage as temporal resolution is required to determine nutrient inputs during summer when eutrophication is most likely to occur.

To overcome these drawbacks, P concentration-flow plots have been used as an integrated indicator of nutrient sources and delivery pathways (Godsey et al., 2009, Basu et al., 2011, Ali et al., 2017). Interpretation of concentration-flow plots is based on the observation that rivers receiving diffuse inputs have a tendency to show an increase in P concentration and load with increasing river flow (Bowes et al., 2009, Jarvie et al., 2010). In contrast, loadings from point sources, such as WWT plants, tend to be relatively constant throughout the year and are generally independent of river flow. Thus, in rivers that are point source dominated, the constant rate of P input results in concentrations that are highest at low flow and that decrease with increasing river flow due to dilution. The benefit of concentration-flow analyses is that they are entirely based on water quality and flow monitoring data that are often relatively easy to obtain. However, the interpretation of nutrient-flow plots to quantify diffuse versus point P inputs, especially seasonally, can be difficult unless these plots are fitted using statistical models (Bowes et al., 2009, Ali et al., 2017).

A load apportionment model (LAM) was developed by Bowes et al. (2008) and uses differences in the mode of P delivery to provide a simple and rapid method for estimating the relative contribution of diffuse versus point-source inputs using only paired nutrient concentration - flow datasets (Jarvie et al., 2010, Bowes et al., 2011, Green et al., 2011). The model has been successfully applied in temperate regions (Bowes et al., 2009, Jarvie et al., 2010, Halliday et al., 2015) but has never been applied to a cold climate region such as the Northern Great Plains (central Canada and northern U.S.A). Here, excessive nutrient loading as a result of human activity has led to eutrophication of downstream waterbodies, including proliferation of harmful algal blooms in the world's 10th largest lake, Lake Winnipeg, Manitoba, Canada (McCullough et al., 2012, Bunting et al., 2016). Application of the LAM in cold climate regions, such as the Northern Great Plains, ought to provide an understanding of potential drivers of the region's eutrophication issues. Such regions differ from mild temperate and tropical regions in that a sizable proportion of total annual precipitation falls as snow during winter, resulting in a hydrological regime that is dominated by snowmelt runoff (Intergovernmental Panel on Climate Change assessment reports, 2018). In addition, unlike mild temperate regions where human population density is often high and wastewater is discharged continuously from treatment facilities, settlements in cold regions tend to be less populated and wastewater inputs are often discrete, with effluent flow occurring over several weeks during summer.

The purpose of this research was to determine the contribution of 'continuous' (point) versus 'flow-dependent' (diffuse) sources of P (total, dissolved, and particulate fractions) to eight sub-watersheds in southern Manitoba, Canada. Small watersheds (< 700 km^2) were selected because they have a clear hydrochemical signal resulting from land use and background geology whereas water quality patterns of larger rivers are an integration of multiple upstream land uses and effluent discharges, which tend to obscure the influences of individual human activities (Jarvie et al., 2010). The present study used the LAM devised by Bowes et al. (2008) to apportion contributions between point and diffuse sources, and determine the influence of seasonality on P inputs to prairie watersheds. Information resulting from application of the model to southern Manitoba streams will assist in identification of P sources and the most effective mitigation strategies to reduce P concentrations and eutrophication risk.

Methods

Site description

This study was conducted in the Red River Valley (RRV) of southern Manitoba, Canada (Fig. 1a). The RRV comprises the historical bed of glacial Lake Agassiz and is characterized by a wide flat plain of fine glacio-lacustrine soils (Yates et al., 2014). The region experiences a cold continental climate with cold winters and warm summers (mean temperatures of -9.3 ^{o}C from November-March and 19 ^{o}C from June-August; 1980-2010 records for Morden, MB; Government of Canada, 2018). Snowmelt typically produces > 60% of annual runoff (Glozier et al., 2006, Dumanski et al., 2015, Rattan et al., 2017), with mineral soils generally frozen at the time of snowmelt and thus not allowing infiltration of water when the snowpack is melting (Fang et al., 2007). Rain precipitation is moderate (average 426 mm/year; 1980-2010 records for Morden, MB; Government of Canada, 2018a) with most spring and summer rain events of high intensity occurring as convective storms (Ali et al., 2017).

Eight sub-watersheds of the Red River (Fig. 1a) were selected to represent a range in agricultural and rural nutrient emitting activities (Fig. 1 b-d). The predominant activities included synthetic fertilizer and manure application and, to a lesser extent, WWT plant inputs. Information on synthetic fertilizer application and rates, crop yield and crop cover were obtained from the Government of Manitoba Agricultural Services Corporation (Manitoba Government, 2018a) for the major crop types (wheat, corn, soybean, sunflower, oats, barley, canola, and flaxseed). The mass of synthetic fertilizer P applied to each sub-watershed was estimated by multiplying the fertilizer application rate by land cover for each crop type, and then summing for all crop types in each sub-watershed (Table 1; Fig. 1b). Livestock nutrient units in each sub-watershed were estimated using 2011 Canadian census data following the methods of Yates et al. (2012). Livestock numbers from each sub-watershed were converted to nutrient unit density using the livestock nutrient coefficient developed by Ontario Ministry of Agriculture, Food and Rural Affairs (2007). The mass of P produced by livestock was estimated for each sub-watershed by multiplying the livestock nutrient units of each livestock type by the coefficients for manure P production obtained from the American Society of Agricultural Engineers (2003) (Table 1; Fig. 1c). The mass of P removed during crop harvest was calculated as the P removal rate (kg/km^2) for each major crop type (Province of Manitoba, 2018; Coordinated financial services Ltd, 2018) multiplied by crop land cover, and then summed for all crop types in each sub-watershed.

In rural areas with low population densities, wastewater lagoons (also called wastewater ponds) are used to receive, hold and treat sewage. Wastewater is piped to a community lagoon where natural processes, usually augmented by artificial aeration, promote biological oxidation. Lagoons release treated wastewater to nearby surface water. In Manitoba, license limits for lagoons restrict flow to a period of weeks or months between June and October, and also identify daily allowable concentration or loading limits (The Environment Act, Manitoba Government, 1988). The location of WWT lagoons was obtained from the Manitoba Land Initiative program (Manitoba Government, 2018). Additional information regarding the estimated number of people served by each lagoon was obtained from Canadian Census 2011 profile (Statistics Canada, 2018) and the Global Anabaptist Mennonite Encyclopedia Online

(GAMEO, 2018). The mass of P discharged from WWT lagoons was estimated by multiplying the population served by each lagoon by a lagoon P removal efficiency coefficient of 3.38 g/capita/day (Chambers et al., 2001) (Table 2; Fig. 1d.).

Water sampling and nutrient loads

Grab water samples were collected during the open-water seasons of 2013 (April 25th- October 31st) and 2014 (April 7th- October 31st) for determination of total P (TP), total dissolved P (TDP), and soluble reactive P (SRP). Sampling protocols were described in detail in Rattan et al. (2018). Briefly, for both years, samples were collected daily during the rising limb and peak of snowmelt, weekly during the falling limb, and biweekly thereafter, for a total of 34 and 42 samples per site in 2013 and 2014, respectively. Sampling ceased in late October when current velocity was <0.001 m^3/s measured over a period of 5 minutes. Samples were not collected during winter as rivers in the Red River Valley (with the exception of the largest) typically freeze to the bottom. All water samples were collected in high density polyethylene bottles, stored at 4^{o}C in a cooler and transported to the Biogeochemical Analytical Services Laboratory, University of Alberta, Edmonton, Alberta. Samples for TDP and SRP were filtered within 24 h of collection and frozen. The remaining P fractions were stored at 4^{o}C and analyzed within a week of sampling. Samples were analyzed using standard methods (American Water Works Association, 1999). Detection limits were 0.001 mg/L for all phosphorus fractions. Particulate P was determined by subtracting total dissolved from total concentrations of P (Yates and Johnes, 2013).

Water levels and temperature were recorded every 30 minutes at each site with a pressure transducer logger (Onset HOBO, Bourne, Massachusetts, USA). Daily discharge, the volume of water moving past the site per day, was estimated from the relationship between water level measured at the site and flow at the nearest Water Survey of Canada (WSC) station (Government of Canada, 2018b) corrected for the difference in watershed area between the WSC station and sample site (Rattan et al., 2018). Nutrient loads were calculated as the product of discharge and nutrient concentration. For dates with missing daily flow or concentration measurements, values were linearly interpolated between the nearest two sampling dates. Comparison of results between methods (linear interpolation versus Stratified Beale Ratio (Schwab et al., 2009)) revealed no statistical differences in estimated loads between methods. Nutrient loads were estimated for each hydrologic season (snowmelt, spring, summer, and fall) and the sampling year (April-October) (Rattan et al., 2019).

Load Apportionment Model

Concentrations of P as TP, TDP, SRP, and PP were modelled individually as a function of stream flow, using the load apportionment model method. The model assumes that the nutrient load from point (L_P) and diffuse (L_D) sources can be modelled as a power-law function of flow (Q) such that the total load (L_T) at the sampling site is a linear combination of the contributions from both sources (Bowes et al., 2008, Halliday et al., 2015):

$$L_T = L_P + L_D \quad \text{where } L_P = A{*}Q \text{ and } L_D = C{*}Q^D \qquad (1)$$

where Q ($m^3\ s^{-1}$) is stream flow, and *A, C,* and *D* are load coefficients determined empirically (Bowes et al., 2014). The A*Q term is the P load originating from constant or continuous sources, which equates to point sources (which, for our study, were WWT lagoons). As these load inputs are constant, they are independent of rainfall (and hence river flow), and therefore this point source term describes a dilution curve as the river flow increases (Figure 2; line A).

The $C*Q^D$ term is the P load from flow-dependent sources, namely diffuse source inputs such as agriculture, groundwater, and septic tank soak-aways (Bowes et al., 2014). The C term equates to the load of diffuse inputs, and D is a gradient term to describe how the load increases with increasing river flow (Figure 2; line B). Because the concentration of P (C_T, mg/L) at a given sampling site can be expressed as the load divided by streamflow:

$$C_T = A*Q^{-1} + C*Q^{D-1} \qquad (2)$$

where *A*, *C*, and *D* are load coefficients to be determined empirically (Bowes et al., 2014), it is possible to solve Eq. (2) by varying the three fitting parameters to produce the closest fit to the empirical data. The values of theA, C and D parameters were determined using the Solver function in Microsoft EXCEL ©. To provide realistic solutions, based on assumptions about the behavior of nutrient sources with flow (Bowes et al., 2008), the D coefficient was constrained to have a value greater than 1, as diffuse load inputs to the river cannot decrease with increasing river flow. The effects of varying A, C, and D load coefficients on P concentration in relation to streamflow are shown in Fig. 2. The point at which the estimated point and diffuse inputs were equal was calculated by:

$$Q_e = (A/C)^{(1/(D))} \qquad (3)$$

Q_e was then used to determine the percentage of time where point sources were the major contributor to total nutrient inputs throughout the sampling period. The nutrient/stream flow relationship was then applied to the daily mean stream flow data set for the monitoring period to calculate the total annual and seasonal load. Results of the model fitting were used to determine the proportion of the total annual, as well as seasonal, nutrient load contributed by point and diffuse inputs (Bowes et al., 2014).

Results

Human activities

In the RRV, land use during our study was dominated by crop (corn, flaxseed, grain, soybean) cultivation and livestock production. Crop cover as a portion of watershed area varied from 59 to 92% across all eight sub-watersheds, with the quantity of synthetic P applied to cropland varying by 5-fold (Table 1, Fig. 1b). Based on estimates of crop yield and average crop P content, the mass of P removed during crop harvest ranged from 155 to 731 t among sub-watersheds. Livestock density expressed as nutrient units exhibited a two-fold range and followed a similar pattern to synthetic P application with the smallest value for both fertilizer application and manure P production observed in the smallest catchment (West Branch La Salle (WBLS) = 61.7 t P as synthetic fertilizer and 32.3 t P as manure) and largest values reported for the largest catchment (Buffalo Channel (BC) = 312 t P as synthetic fertilizer and 225 t P as manure) (Table 1; Fig. 1c). Removal of P as a result of crop harvest exceeded synthetic P application for all sub-watersheds. Combining both synthetic and manure P (i.e., assuming all manure P was applied to cropland) did not result in a surplus of P within the sub-watersheds: P uptake by crops still exceeded P application (Table 1).

In addition to agricultural land cover, the RRV is characterized by comparatively low human population settled in scattered farmhouses (served by septic systems), small towns (served by public WWT lagoons) and religious colonies (served by private WWT lagoons). Loads of P associated with lagoon WWT discharge ranged from 0 (for watersheds with no lagoons) to 2.5 t/y for the watershed with the largest population served by a WWT lagoon (Table 2; Fig. 1d).

Phosphorus dynamics

Phosphorus concentrations in the eight streams ranged from 0.02-3.5 mg/L TP, 0.02-3.2 mg/L TDP, 0.01-2.9 mg/L SRP, and 0.01-3.0 mg/L PP. For both years, mean annual TP concentrations were greatest in WBLS followed by Dead Horse Creek (DHC) (Table S1). Mean annual TP concentrations were lowest in Elm Creek (EC) in 2013 and Shannon Creek (SC) in 2014. Although TP concentrations varied among sites, only Hespeler Drain (HD) showed a significant difference ($p<0.05$) in TP between years, being lower in 2014 compared to 2013 (Table S1). Similar to TP, the sub-watersheds showed variability in TDP and PP concentrations among sites in a given year. However, only two streams had mean annual TDP or PP concentrations that differed significantly ($p<0.05$) between years: Buffalo Creek (BC) had a higher mean annual concentration of TDP in 2014 compared to 2013 while Shannon Creek (SC) had a greater mean concentration of PP in 2013 compared to 2014 (Table S1).

Phosphorus loads and yields ranged from 2.2 - 31 t/y and 0.0061-0.11 t/km^2 TP; 1.2-17 t/y and 0.0041-0.088t/km^2 TDP; 0.59-16 t/y and 0.0021-0.061 t/km^2 SRP; and 0.52-23 t/y and 0.0031-0.082 t/km^2 PP (Table S1). Comparison between years showed that mean TP and PP loads and yields were significantly greater ($p<0.05$) in 2013 for medium to large sub-watersheds (180-626 km^2), notably Tobacco Creek (TC), DHC, SC, BC, and HD. Moreover, in the case of the TC and DHC sub-watersheds, TDP and SRP loads and yields were also significantly greater ($p<0.05$) in 2013. Only one sub-watershed (EC with a watershed area of 602 km^2) showed greater TP, TDP, and SRP loads and yields in 2014.

During snowmelt, TP concentrations were significantly greater ($p<0.05$) for the DHC, SC, and HD sub-watersheds in 2013 (Table S2). TP concentrations for the EC and BCD sub-watersheds were significantly greater ($p<0.05$) in 2014 compared to 2013. TDP concentrations were significantly greater in 2013 compared to 2014 for WBLS and HD sub-watersheds. For EC and SC sub-watersheds, SRP concentrations were significantly greater ($p<0.05$) in 2014; and PP concentrations were significantly greater ($p<0.05$) for the DHC (0.33 mg/L), SC (0.82 mg/L), and BC (0.23 mg/L) sub-watersheds in 2013. Comparison of loads and yields showed that snowmelt, TP and PP loads and yields were, on average, greater ($p<0.05$) in 2013 for medium to large sub-watersheds (180-626 km^2), a pattern similar to the annual P loads and yields (S2). In addition, the TC sub-watershed dissolved P loads and yields were significantly greater ($p<0.05$) in 2013.

During the summer period, TP concentrations were greater for the EC and DHC sub-watersheds in 2014 (Table S3). Concentrations were also greater ($p<0.05$) in summer 2014 compared to summer 2013 for TP in the EC, TC, DHC, SC, BC, and HD sub-watersheds and for SRP for all sub-watersheds, most notably the WBLS sub-watershed (0.0009 mg/L in 2013 compared to 0.84 mg/L in 2014). Variation in P loads and yields among sub-watersheds differed from patterns observed for P concentrations (Table S3). Notably, loads and yields of all P fractions were greater ($p<0.05$) during summer 2013 for the TC, DHC, SC, BC, and HD sub-watersheds yet greater during summer 2014 for the EC, BCD, and WBLS (except for PP) sub-watersheds.

Load apportionment model output

Annual contributions

The load apportionment model produced "realistic" fits for the majority (60 of 64) of the annual relationships between P concentration and streamflow (Table S4). Moreover, annual loads of P estimated by the model (Table 3) were in agreement with observed loads (Table S1): expected: observed ratios were 1.01±0.021, 1.09±0.081, 1.07±0.041 and 1.10±0.016 for TP, TDP, SRP and PP, respectively (mean±SE; data combined for both years). Realistic model fits could not, however, be achieved for PP for the EC sub-watershed in both 2013 and 2014, for PP in the BCD sub-watershed in 2014, and for TP in the BCD sub-watershed in 2013 (Table S4). In the case of the unsuccessful PP models, the concentration-flow relationships had considerable scatter such that the best-fit model was a horizontal line through the data, suggesting that the model predicted the average P concentration for all flow rates.

The parameter values derived from the load apportionment model showed an overwhelming dominance of diffuse P source contribution (Table 3). This was also evident from the concentration-flow relationships, where only C and D parameters (i.e., A = 0) were required to successfully model the empirical data for all sites except WBLS (all P forms in both years), DHC (SRP only for both years), and SC and BC (PP in 2014 only for both sites) (Table S4). Examination of concentration versus flow plots confirmed these findings: all tributaries except WBLS and DHC showed an increase in P concentration with increasing flow, consistent with 100% dominance by diffuse sources (Figures 3 and 4, sub-watersheds EC and HD as examples). In the case of WBLS and DHC, P concentrations showed considerable scatter and often attained peak values at low stream flows, consistent with dilution of a constant point source input (Figures 3 and 4, sub-watersheds WBLS and DHC). In terms of contribution to annual loads, point sources accounted for 11 and 9% of the TP load, 7 and 12% of the TDP load, 8 and 14% of the SRP load, and 30 and 18% of the PP load for 2013 and 2014, respectively, for the WBLS sub-watershed. For the other watersheds with point source inputs, annual contributions were 3-4% for SRP for sub-watershed DHC and 6-7% for PP for sub-watersheds SC and BC (Table 3).

Seasonal contributions

As was observed for the annual data, diffuse sources were also the predominant source of P to all eight sub-watersheds during both snowmelt (Table 4) and summer (Table 5). Similar to results from the annual load apportionment model, the seasonal predicted loads (Tables 4 and 5) were in agreement with observed loads (Tables S2 and S3): observed expected ratios were 1.01 ±0.056, 1.05 ± 0.031, 1.04 ± 0.022, 0.992 ± 0.12 for TP, TDP, SRP and PP, respectively, during snowmelt and similarly 1.05 ± 0.015, 1.04 ± 0.026, 1.02 ± 0.054, 1.09 ± 0.025 for TP, TDP, SRP, and PP, respectively, during summer.

For snowmelt, "realistic" fits were attained for all but 3 of the 64 relationships between P concentration and streamflow (Table S5). The three exceptions occurred in the two sub-watersheds without WWT lagoons (namely HD and BCD), with the concentration-flow plots showing more scatter and the models producing only a horizontal line indicative of no optimal fit. With the exception of WBLS, snowmelt P loads in all sub-watersheds were derived solely from diffuse sources (Table 4). In the case of WBLS, point sources were a minor contributor (0 - 11%) to snowmelt P loads in 2013 but a major contributor (52-100%) to snowmelt P loads in 2014. The point-source contribution to snowmelt P loads for WBLS were consistent with the values of the A parameter in the load apportionment models: 2.1, 11, 0.54 and 0.0 in 2013 compared to 81, 113, 89, and 211 in 2014 for TP, TDP, SRP and PP, respectively (Table S5).

Thus, during snowmelt, and particularly snowmelt 2014, point sources were a contributor to P loads for the WBLS sub-watershed.

For summer, "realistic" fits were attained for all 64 relationships between P concentration and streamflow (Table S6). For both the 2013 and 2014 summers, sub-watersheds WBLS and DHC were identified as having point-source inputs for TP, TDP and SRP; DHC also showed point-source inputs of PP in summer 2013 (Table 5). For these two sub-watersheds, point sources represented 4-47% of the TP, TDP or SRP summer load. Consistent with the high point-source contribution, the WBLS and DHC sub-watersheds had the highest A parameter values: 44, 33, and 62 for WBLS and 88, 15, and 63 for DHC for TP, TDP and SRP, respectively (Table S6). The A parameter values were, however, significantly ($p<0.05$) less in summer 2014 compared to summer 2013 for both sub-watersheds. In addition to these two sub-watersheds with substantial point source inputs, BC and HD also showed minor point source-inputs in 2014 (1% of the TDP load and, in the case of HD only, 1% of the TP load) (Table 5).

Discussion

Modeling of phosphorus loads using concentration and flow data showed that the Load Apportionment Model (Bowes et al., 2008) produced, on average, realistic estimates of diffuse and point-source inputs for watersheds in a sparsely-populated cold-climate region of southern Manitoba, Canada. The LAM predicted P loads that agreed, on average, with observed loads: expected: observed ratios for the eight study sites averaged 0.99-1.10 for the four P fractions and three time periods. Moreover, the LAM identified that all eight sub-watersheds were predominately supplied by P from diffuse sources. This finding is consistent with that fact that southern Manitoba, though characterized by a cold continental climate, is a major agricultural region with land use dominated by crop cultivation and livestock production (Manitoba Government, 2018). Although the LAM has never before been applied to a cold climate region, successful model results have been achieved for temperate rural areas. For example, application of the LAM to rural catchments in England showed that point-source P loads were minimal in low agricultural intensity catchments, compared to high intensity arable catchments (Jarvie et al., 2010). Similarly, Halliday et al. (2015) found that for an urban catchment located in The Cut (upstream of the River Thames, England), the LAM accurately identified that human effluent accounted for a high proportion (50%) of the annual P load. Observations that the LAM correctly identified the source of P inputs to both temperate streams with a mix of urban and agricultural activities (e.g., Jarvie et al., 2010, Halliday et al., 2015) and cold-climate rural watersheds of southern Manitoba (this study) supports application of this model for distinguishing point and diffuse source P inputs.

While the LAM estimated that diffuse source inputs represented 70-100% of the annual P load (TP, TDP, SRP and PP), diffuse sources inputs comprised a broader range of 0-100% during snowmelt and 53-100% during summer. Conversely, point source inputs contributed 0-30% annually compared to 0-100% during snowmelt and 0-47% during summer. The broader range in seasonal compared to annual contributions is indicative of changes in P sources among seasons. For our sub-watersheds, this seasonal variability was driven by summer release of wastewater, particularly to DHC (the sub-watershed with wastewater inputs at least double that of the others; Table 2). For this sub-watershed, the LAM solutions mirrored the typical pattern of effluent release in cold climate rural regions: during snowmelt, diffuse sources supplied the entire P load whereas during summer when sewage lagoons are permitted to discharge wastewater, point source inputs increased. In contrast, seasonality in nutrient apportionment in temperate regions is generally associated with high flow events, such as multi-day precipitation events, which generate a higher proportion of diffuse P input relative to continuous P sources (Jarvie et al., 2010, Greene et al., 2011, Halliday et al., 2015).

Yet while strong seasonal variability in nutrient source apportionment was observed for the sub-watershed with the greatest wastewater input (DHC), model outputs for the sub-watershed with the smallest wastewater input (namely WBLS) indicated sizable point source contributions. In fact, point-source inputs to WBLS comprised 17-40% of the P load (TP, TDP, SRP and PP) during summer (2013 and 2014) and an even greater share of 52-100% during snowmelt 2014 (although a low share of 3-11% during snowmelt 2013). The quantification by the LAM of a sizable point-source input during summer and also during snowmelt indicates an unaccounted P source. This fugitive P could result from release, seepage or leakage from a WWT lagoon or a slurry pond used to store livestock waste, or runoff from farmyards or manure piles (e.g., Jarvie et al., 2010). The observation that 100% of the 2014 snowmelt PP load in the WBLS sub-watershed was derived from point sources suggests that the fugitive P source during snowmelt 2014 was particulate barnyard wastes (i.e., manure, bedding and litter, wasted feed). In contrast, the majority of effluent discharged from WWT lagoons, including the lagoon on DHC, is in dissolved form (Carlson et al., 2013). Moreover, the fact that WBLS had the highest livestock density and the finding that livestock density is a significant predictor of TP concentration in these streams (Rattan et al., 2017) suggest that the unaccounted fugitive P source to WBLS is direct delivery of livestock manure, farmyard runoff, or a slurry stream.

In conclusion, load apportionment modelling (LAM) of P sources can provide a basis for identification of major contributing sources, detection of unknown sources and, in turn, development of effective mitigation strategies to reduce P concentrations and eutrophication risk. Previous studies have shown that crop cultivation, livestock density, and residential wastewater (Yates et al., 2012, Ali et al., 2017, Rattan et al., 2017) can be important P sources to waterbodies and drivers of eutrophication to downstream waterbodies such as Lake Winnipeg. The LAM applied in this study provided a cost-effective solution for quantifying diffuse versus point sources of P in terms of timing, duration, and magnitude. Application of the LAM often includes the assumption that point source inputs are constant through the year, an assumption which is generally true in temperate regions but is likely not the case in cold-climate, rural regions. By applying the LAM separately for each hydrologic period, we produced reliable outputs that identified the relative contribution of diffuse versus point sources for both the snowmelt and summer periods. This will allow land managers to focus P management efforts on the right sources at the right time – key elements of the 4Rs of nutrient management (applying the right nutrient source at the right rate, at the right time and in the right place).

Acknowledgments

We thank Ross MacKay, Zoey Duggan, Jon Challis, Julie Anderson, and Alistair Brown for their contributions to field data collection. This project was funded by Environment and

Climate Change Canada through the Lake Winnipeg Basin Initiative and a National Science Engineering Research Council (NSERC) Visiting Fellowship Award to K.J.R.

References

Ali, G., Wilson, H., Elliott, J., Penner, A., Haque, A., Ross, C., Rabie, M., 2017. Phosphorus export dynamics and hydrobiogeochemical controls across gradients of scale, topography and human impact. Hydrol. Process. 31, 3130-3145

American Society of Agricultural Engineers. 2003. Manure production and characteristics. American Society of Agricultural Engineers D384.1 FEB03.

American Public Health Association, American Water Works Association, Water Environment Federation, 1999. Standard Methods for the Examination of Water and Wastewater.

Basu, N. B., Thompson, S. E., Rao, P. S. C., 2011. Hydrologic and biogeochemical functioning of intensively managed catchments: A synthesis of top-down analyses. Water Resour. Res. 47, 10-23.

Bowes, M. J., Hilton, J., Irons, G. P., Hornby, D. D., 2005a. The relative contribution of sewage and diffuse phosphorus sources in the River Avon catchment, southern England: implications for nutrient management. Sci. Tot. Environ. 344, 67-81.

Bowes, M. J., House, W. A., Hodgkinson, R. A., Leach, D. V., 2005b. Phosphorus–discharge hysteresis during storm events along a river catchment: the River Swale, UK. Water Res. 39, 751-762.

Bowes, M. J., Leach, D. V., House, W. A., 2005. Seasonal nutrient dynamics in a chalk stream: the River Frome, Dorset, UK. Sci. Tot. Environ., 336, 225-241.

Bowes, M. J., Smith, J. T., Jarvie, H. P., Neal, C., 2008. Modelling of phosphorus inputs to rivers from diffuse and point sources. Sci. Tot. Environ., 395, 125-138.

Bowes, M. J., Smith, J. T., Jarvie, H. P., Neal, C., Barden, R., 2009. Changes in point and diffuse source phosphorus inputs to the River Frome (Dorset, UK) from 1966 to 2006. Sci. Tot. Environ., 407, 1954-1966.

Bowes, M. J., Neal, C., Jarvie, H. P., Smith, J. T., Davies, H. N., 2010. Predicting phosphorus concentrations in British rivers resulting from the introduction of improved phosphorus removal from sewage effluent. Sci. Tot. Environ., 408, 4239-4250.

Bowes, M. J., Smith, J. T., Neal, C., Leach, D. V., Scarlett, P. M., Wickham, H. D., Davies, C. E., 2011. Changes in water quality of the River Frome (UK) from 1965 to 2009: Is phosphorus mitigation finally working? Sci. Tot. Environ., 409, 3418-3430.

Bowes, M. J., Gozzard, E., Johnson, A. C., Scarlett, P. M., Roberts, C., Read, Wickham, H. D., 2012. Spatial and temporal changes in chlorophyll-a concentrations in the River Thames basin, UK: Are phosphorus concentrations beginning to limit phytoplankton biomass? Sci. Tot. Environ., 426, 45-55.

Bowes, M. J., Jarvie, H. P., Naden P. S., Old, G. H., Scarlett, P. M., Roberts, C., Armstrong, L. K., Harman, S. A., Wickham, H. D., Collins, A. L., 2014. Identifying priorities for nutrient mitigation using river concentration–flow relationships: The Thames basin, UK. J. Hydrol., *517*, 1-12.

Brooks, G., 2017. Red River Valley, Manitoba: The geomorphology of a low-relief, flood-prone prairie landscape, in Slaymaker, O. (Ed), Landscape and Landforms of Western Canada. Natural Resources Canada, Geological Survey of Canada, pp 143-155.

Bunting, L., Leavitt, P. R., Simpson, G. L., Wissel, B., Laird, K. R., Cumming, B. F., St. Amand, A., Engstrom, D. R., 2016. Increased variability and sudden ecosystem state change in Lake Winnipeg, Canada, caused by 20th century agriculture. Limnol. Oceanogr., 61, 2090-2107.

Burt, T. P., Johnes, P. J., 1997. Managing water quality in agricultural catchments. Trans. Inst. Br. Geogr., 22, 61-68.

Carlson, J.C., Anderson, J.C., Low, J.E., Cardinal, P., MacKenzie, S.D., Beattie, S.A., Challis, J.K., Bennett, R.J., Meronek, S.S., Wilks, R.P.A., Buhay, W.M., Wong, C.S., Hanson, M.L., 2013. Presence and hazards of nutrients and emerging organic micropollutants from sewage lagoon discharges into Dead Horse Creek, Manitoba, Canada. Sci. Tot. Environ., 445-446, 64-78.

Chambers, P.A., Guy, M., Roberts, S.E., Charlton, M.N., Kent, R., Gagnon, C., Grove, G., Foster, N., 2001. Nutrients and their impact on the Canadian environment. Agricultural and Agri-Food Canada, Environment Canada, Fisheries and Oceans Canada, Health Canada and Natural Resources Canada.

Co-Ordinated Financial Services Ltd. 2018. http://www.farmbooks.ca/Converter.html. Accessed on June 15, 2018

Dumanski, S., Pomeroy, J.W., Westbrook, C. J., 2015. Hydrological regime changes in a Canadian Prairie basin. Hydrol. Process., *29*, 3893-3904.

Edwards, A.C., Withers, P.J.A., 2007. Linking phosphorus sources to impacts in different types of water body. Soil Use Manag., 23, 133–143.

Elliott, J., 2013. Evaluating the potential contribution of vegetation as a nutrient source in snowmelt runoff. Can. J. Soil. Sci. 93, 435-443.

Fang, X., Pomeroy, J.W., 2007. Snowmelt runoff sensitivity analysis to drought on the Canadian prairies. Hydrol. Process., 21, 2594-2609.

Global Anabaptist Mennonite Encyclopedia Online (GAMEO), 2018. Accessed on March 05, 2018. https://gameo.org/index.php?title=Welcome_to_GAMEO

Glozier, N. E., Elliott, J. A., Holliday, B., Yarotski, J., Harker, B., 2006. Water quality characteristics and trends in a small agricultural watershed: South Tobacco Creek, Manitoba, 1992–2001. Environment Canada, Ottawa, ON.

Godsey, S. E., Kirchner, J. W., Clow, D. W., 2009. Concentration discharge relationships reflect chemostatic characteristics of US catchments. Hydrol. Process., 23,1844–1864. https://doi.org/ 10.1002/hyp.7315.

Government of Canada., 2018a. Historical Climate Data for Morden, Manitoba. Accessed: June 1st 2015, http://climate.weather.gc.ca/historical_data/search_historic_data_stations_e.html?searchType=stnName&timeframe=1&txtStationName=Morden&searchMethod=contains&optLimit=yearRange&StartYear=1840&EndYear=2014&Year=2014.

Government of Canada., 2018b. Real-Time Hydrometric Data Search, Manitoba. Accessed: June 1st 2015, https://wateroffice.ec.gc.ca/search/real_time_results_e.html?search_type=province&province=MB&gross_drainage_operator=%3E&gross_drainage_area=&effective_drainage_operator=%.

Greene, S., Taylor, D., McElarney, Y. R., Foy, R. H., Jordan, P., 2011. An evaluation of catchment-scale phosphorus mitigation using load apportionment modelling. Sci. Tot. Environ., 409, 2211-2221.

Halliday, S. J., Skeffington, R. A., Wade, A. J., Bowes, M. J., Gozzard, E., Newman, J. R., Loewenthal, M., Palmer-Felgate, E. J., Jarvie, H. P., 2015. High frequency water quality monitoring in an urban catchment: hydrochemical dynamics, primary production and implications for the Water Framework Directive. Hydrol. Process., 29: 3388-3407.

Heard J., Hay, D., 2010. Nutrient content, uptake pattern and carbon: nitrogen ratios of Prairie crops. Manitoba Agriculture, Food and Rural Initiatives, pp 1-10.

Intergovernmental Panel on Climate Change assessment reports., 2018. Accessed: March 16th 2018. http://www.ipcc.ch/ipccreports/tar/wg2/index.php?idp=169

Jarvie, H. P., Jürgens, M. D., Williams, R. J., Neal, C., Davies, J. J., Barrett, C., White, J., 2005. Role of river bed sediments as sources and sinks of phosphorus across two major eutrophic UK river basins: the Hampshire Avon and Herefordshire Wye. J. Hydrol., 304, 51-74.

Jarvie, H. P., Withers, P. J. A., Bowes, M. J., Palmer-Felgate, E. J., Harper, D. M., Wasiak, K. Neal, M,. 2010. Streamwater phosphorus and nitrogen across a gradient in rural–agricultural land use intensity. Agric. Ecosyst. Environ., 135, 238-252.

Johnes, P. J., Heathwaite, A. L., 1997. Modelling the impact of land use change on water quality in agricultural catchments. Hydrol. Process., 11, 269-286.

Manitoba Government, 2018a Manitoba Agricultural Services Corporation – Agricultural Statistic Tables. Accessed: July 5th 2018, http://www.gov.mb.ca/agriculture/markets-and-statistics/statistics-tables/index.html.

Manitoba Government, 2018b. Manitoba Soil Fertility Guide. Appendix 1. Accessed: February 20th 2018. https://www.gov.mb.ca/agriculture/crops/soil-fertility/pubs/phosphorus-fertilization-strategies-for-manitoba.pdf.

McCullough, GK., Page, S.J., Hesslein, R.H., Stainton, M.P., Kling, H.J., Salki, A.G., Barber, D.G., 2012. Hydrological forcing of a recent trophic surge in Lake Winnipeg. J. Great. Lakes Res., 38, 95-105.

Ontario Ministry of Agriculture, Food, and Rural Affairs, 2007. Nutrient management Protocol. Ontario Ministry of Agriculture, Food, and Rural Affairs.

Palviainen, M., Laurén, A., Launiainen, S., Piirainen, S., 2016. Predicting the export and concentrations of organic carbon, nitrogen and phosphorus in boreal lakes by catchment characteristics and land use: A practical approach. Ambio, 45, 933-945.

Rattan, K. J., Corriveau, J. C., Brua, R. B., Culp, J. M., Yates, A. G., & Chambers, P. A., 2017. Quantifying seasonal variation in total phosphorus and nitrogen from prairie streams in the Red River Basin, Manitoba Canada. Sci. Tot. Environ., *575*, 649-659.

Rattan K.J., Blukacz-Richards E.A., Yates A.G., Culp, J.M., Chambers P.A., 2019. Hydrological variability affects nitrogen and phosphorus export from streams of the Northern Great Plains. J. Hydrol. Reg. Studies, 21, 110-125.

Schwab, D. J., Beletsky, D., DePinto, J., Dolan, D. M., 2009. A hydrodynamic approach to modeling phosphorus distribution in Lake Erie. J. Great Lakes Res., 35, 50-60.

Sharpley, A.N., Chapra, S.C., Wedepol, R., Sims, J.T., Daniel, T.C., Reddy, K.R., 1994. Managing agricultural phosphorus for protection of surface waters: issues and options. J. Environ. Qual., 23, 437–451.

Smith, V. H., Schindler, D. W., 2009. Eutrophication science: where do we go from here? Trends Ecol. Evol., 24, 201-207.

Statistics Canada, 2011 Canadian census. Accessed on March 16th 2018. https: //www12.statcan.gc.ca/census-recensement/2011/dp-pd/prof/index.cfm?Lang=Eng

Yates, C. A., Johnes, P. J., 2013. Nitrogen speciation and phosphorus fractionation dynamics in a lowland Chalk catchment. Sci. Tot. Environ., 444, 466-479.

Yates, A. G., Culp, J. M., Chambers, P. A., 2012. Estimating nutrient production from human activities in sub-catchments of the Red River, Manitoba. J. Great Lakes Res., 38, 106-114.

Yates, A. G., Brua, R. B., Corriveau, J., Culp, J. M., Chambers, P. A., 2014. Seasonally driven variation in spatial relationships between agricultural land use and instream nutrient concentrations. River Res. Appl., 30, 476-493.

Figures

Figure 1 a-d. Location (a) of the eight sub-watersheds in the Red River Valley of southern Manitoba. Also shown are the quantities of (b) synthetic phosphorus (P) fertilizer applied to crops, (c) livestock manure P produced, and (d) total P (TP) released from wastewater treatment (WWT) plants for each study watershed. Location of WWT plants in sub-watersheds are identified by brown circles in panel (d).

Figure 2. Example of relationship between phosphorus concentration (P mg/L) and streamflow (m^3/s) for (a) point source dominated system – inverse relationship, (b) diffuse source dominated system – exponential relationship and (c) combined point and diffuse sources –“ U” shaped relationship (adapted from Greene et al. 2011).

Figure 3. Annual (2013) relationships between total phosphorus (TP), total dissolved phosphorus (TDP), soluble reactive phosphorus (SRP), and particulate phosphorus (PP) concentrations and stream flow for selected study sites in the Red River Valley of southern Manitoba: (a-d) West Basin La Salle (WBLS), (e-h) Dead Horse Creek (DHC), (i-l) Elm Channel (EC), and (m-p) Hespeler Drain (HD). Measured P concentrations are depicted as black circles and estimated P concentrations derived from the load apportionment model are depicted as red circles.

Figure 4 Annual (2014) relationships between TP, TDP, SRP, and PP concentrations and stream flow for selected study sites in the RRV of southern Manitoba: (a-d) West Basin La Salle (WBLS), (e-h) Dead Horse Creek (DHC), (i-l) Elm Channel (EC), and (m-p) Hespeler Drain (HD). Measured P concentrations are depicted as black circles and estimated P concentrations derived from the load apportionment model are depicted as red circles.

Figure 5 Seasonal (snowmelt 2013 and 2014) relationships between TP and SRP concentrations and stream flow for selected study sites in the RRV of southern Manitoba: (a-d) West Basin La Salle (WBLS), (e-h) Dead Horse Creek (DHC), (i-l) Elm Channel (EC), and (m-p) Hespeler Drain (HD). Measured P concentrations are depicted as black circles and estimated P concentrations derived from the load apportionment model are depicted as red circles.

Figure 6 Seasonal (summer 2013 and 2014) relationships between TP and SRP concentrations and stream flow for selected study sites in the RRV of southern Manitoba: (a-d) West Basin La Salle (WBLS), (e-h) Dead Horse Creek (DHC), (i-l) Elm Channel (EC), and (m-p) Hespeler Drain (HD). Measured P concentrations are depicted as black circles and estimated P concentrations derived from the load apportionment model are depicted as red circles.

Table. 1 Diffuse P sources in the Red River Valley, Manitoba, Canada. P applied as synthetic fertilizer and P removal rates were obtained from the Manitoba soil fertility guide (https://www.gov.mb.ca/agriculture/crops/soil-fertility/pubs/phosphorus-fertilization-strategies-for-manitoba.pdf). Livestock nutrient units were calculated using the livestock nutrient coefficient developed by Ontario Ministry of Agriculture, Food and Rural Affairs (2007). Coefficients for calculating P content in manure were obtained from Manure production and characteristics, American Society of Agricultural Engineers (2003). Residual P remaining in sub-catchment was calculated as synthetic P applied + Manure P – P removed by crops. T = Tonnes.

Sub-Watershed	Code	Catchment Area (km^2)	Crop			Livestock		Residual P
			% crop cover	Synthetic P applied (T)	P removed in harvest (T)	Nutrient Units (NU)	Manure P (T)	(Synthetic P + Manure P) – (P harvest) (T)
Elm	EC	602	70	273	605	15.9	180	-152
Tobacco	TC	248	71	182	420	22.1	142	-96.0
Dead Horse	DHC	217	69	111	255	22.2	87.8	-56.2
Shannon	SC	279	65	146	342	21.9	112	-84.0
Buffalo	BC	626	59	312	731	18.8	225	-194
West Branch La Salle	WBLS	65	87	61.7	143	25.1	32.3	-49.0
Hespeler	HD	180	69	88.5	206	23.4	77.3	-40.2
Big Coulee	BCD	84	92	70.1	155	36.8	36.9	-48.0

Table 2. The number of waste water lagoons in eight sub-watersheds of southern Manitoba and their estimated total phosphorus (TP) release. The location of private and public lagoons were obtained from the Manitoba Land Initiative Program (http://mli2.gov.mb.ca/environment/index.html).

Sub-Watershed	Code	Catchment area (km^2)	Wastewater Lagoons (number)			Population served [1,2]	TP	
			Public	Private	Total		Load (T)	Yield (T/km^2)
Elm	EC	602	1	2	3	925	0.277	0.0004
Tobacco	TC	248	1	2	3	248	0.070	0.0002
Dead Horse	DHC	217	1	0	1	8668	2.460	0.0120
Shannon	SC	279	1	0	1	623	0.177	0.0007
Buffalo	BC	626	1	0	1	574	0.163	0.0003
West Branch La Salle	WBLS	65	0	1	1	135	0.038	0.0021
Hespeler	HD	180	0	0	0	0	0.000	0.000
Big Coulee	BCD	84	0	0	0	0	0.000	0.000

[1] Data obtained from Manitoba Census profile 2011 http://www.12.statcan.ca

[2] Data obtained from Global Anabaptist Mennonite Encyclopedia Online http://gameo.org

Table 3 Estimated diffuse source (DS) and point source (PS) contributions to annual (2013 and 2014) P loads and yields, and the proportion of time that P loads were point source dominated. Values derived from load apportionment modelling.

Sub-watershed	2013 Annual						2014 Annual					
	DS load (t)	PS load (t)	DS yield (t/km^2)	DS load as % of annual load	PS load as % of annual load	% time PS load dominant	DS load (t)	PS load (t)	DS yield (t/km^2)	DS load as % of annual load	PS load as % of annual load	% time PS load dominant
TP												
WBLS	4.7	0.99	0.072	89	11	41	6.6	0.84	0.10	91	9	1
EC	9.7	0.0	0.016	100	0	0	20	0.0	0.033	100	0	0
TC	22	0.0	0.063	100	0	0	2.4	0.0	0.0070	100	0	0
DHC	15	0.0	0.056	100	0	0	3.2	0.0	0.015	100	0	0
SC	32	0.0	0.18	100	0	0	3.7	0.0	0.013	100	0	0
BC	28	0.0	0.13	100	0	0	15	0.0	0.004	100	0	0
HD	15	0.0	0.023	100	0	0	3.1	0.0	0.017	100	0	0
BCD	2.1	0.0	0.025	100	0	0	2.4	0.0	0.029	100	0	0
TDP												
WBLS	5.8	0.084	0.089	93	7	2	3.4	0.92	0.052	88	12	2
EC	6.8	0.0	0.011	100	0	0	15	0.0	0.026	100	0	0
TC	10	0.0	0.030	100	0	0	1.4	0.0	0.004	100	0	0
DHC	8.3	0.0	0.030	100	0	0	1.5	0.0	0.007	100	0	0
SC	3.8	0.0	0.021	100	0	0	2.8	0.065	0.009	100	0	0
BC	18	0.0	0.083	100	0	0	13	0.016	0.002	100	0	0
HD	13	0.0	0.072	100	0	0	2.2	0.0	0.012	100	0	0
BCD	1.2	0.0	0.015	100	0	0	1.8	0.0	0.021	100	0	0

SRP												
WBLS	3.2	0.27	0.049	92	8	9	4.0	0.49	0.061	86	14	34
EC	5.7	0.0	0.009	100	0	0	11	0.0	0.019	100	0	0
TC	7.7	0.0	0.022	100	0	0	0.73	0.0	0.002	100	0	0
DHC	5.9	0.19	0.027	97	3	10	2.6	0.10	0.012	96	4	11
SC	3.3	0.0	0.018	100	0	0	2.6	0.011	0.009	100	0	0
BC	16	0.0	0.074	100	0	0	13	0.0	0.001	100	0	0
HD	5.8	0.0	0.009	100	0	0	1.9	0.0	0.010	100	0	0
BCD	0.57	0.0	0.007	100	0	0	1.4	0.0	0.017	100	0	0
PP												
WBLS	1.1	0.33	0.016	70	30	73	1.2	0.22	0.018	82	18	46
EC	3.9	0.0	0.006	100	0	0	5.7	0.0	0.009	100	0	0
TC	11	0.0	0.033	100	0	0	1.1	0.0	0.003	100	0	0
DHC	7.9	0.0	0.028	100	0	0	1.2	0.0	0.005	100	0	0
SC	23	0.0	0.13	100	0	0	1.1	0.090	0.004	94	6	0
BC	9.6	0.0	0.045	100	0	0	2.6	0.23	0.002	93	7	0
HD	8.8	0.0	0.014	100	0	0	1.1	0.0	0.006	100	0	0
BCD	0.58	0.0	0.007	100	0	0	0.53	0.0	0.006	100	0	0

Table 4. Estimated diffuse and point contributions to snowmelt (2013 and 2014) P loads, P yields, and the proportion of time that P loads are point source dominated. Values derived from load apportionment modelling.

Sub-watershed	2013 Snowmelt						2014 Snowmelt					
	DS load (t)	PS load (t)	DS yield (t/km^2)	DS load as % of annual load	PS load as % of annual load	% time PS load dominant	DS load (t)	PS load (t)	DS yield (t/km^2)	DS load as % of annual load	PS load as % of annual load	% time PS load dominant
TP												
WBLS	3.7	0.25	0.056	94	6	11	0.54	1.5	0.008	26	74	86
EC	7.8	0.0	0.013	100	0	0	11	0.0	0.019	100	0	0
TC	14	0.0	0.042	100	0	0	1.5	0.0	0.004	100	0	0
DHC	8.3	0.0	0.038	100	0	0	2.5	0.0	0.012	100	0	0
SC	25	0.0	0.090	100	0	0	3.5	0.0	0.012	100	0	0
BC	20	0.0	0.033	100	0	0	14	0.0	0.022	100	0	0
HD	11	0.0	0.063	100	0	0	3.0	0.0	0.017	100	0	0
BCD	0.80	0.0	0.010	100	0	0	0.86	0.0	0.010	100	0	0
TDP												
WBLS	3.1	0.38	0.047	89	11	28	0.81	0.76	0.012	48	52	55
EC	6.4	0.0	0.011	100	0	0	8.7	0.0	0.014	100	0	0
TC	6.9	0.0	0.020	100	0	0	1.1	0.0	0.003	100	0	0
DHC	2.7	0.0	0.013	100	0	0	3.0	0.0	0.010	100	0	0
SC	2.9	0.0	0.010	100	0	0	2.3	0.0	0.008	100	0	0
BC	14	0.0	0.022	100	0	0	13	0.0	0.021	100	0	0
HD	11	0.0	0.063	100	0	0	1.9	0.0	0.011	100	0	0
BCD	0.62	0.0	0.007	100	0	0	0.69	0.0	0.008	100	0	0
SRP												
WBLS	2.4	0.084	0.037	97	3	0	0.75	0.59	0.020	45	55	45
EC	5.5	0.0	0.009	100	0	0	7.2	0.0	0.011	100	0	0
TC	5.3	0.0	0.015	100	0	0	0.54	0.0	0.001	100	0	0

DHC	2.1	0.0	0.010	100	0	0	2.1	0.0	0.010	100	0	0
SC	2.6	0.0	0.010	100	0	0	2.2	0.0	0.008	100	0	0
BC	12	0.0	0.020	100	0	0	12	0.0	0.020	100	0	0
HD	5.0	0.0	0.028	100	0	0	1.7	0.0	0.009	100	0	0
BCD	0.34	0.0	0.004	100	0	0	0.47	0.0	0.005	100	0	0
PP												
WBLS	0.71	0.0	0.011	100	0	0	0.0	0.93	0.014	0	100	100
EC	2.0	0.0	0.003	100	0	0	2.1	0.0	0.0035	100	0	0
TC	7.4	0.0	0.021	100	0	0	0.49	0.0	0.001	100	0	0
DHC	6.9	0.0	0.032	100	0	0	0.81	0.0	0.003	100	0	0
SC	21	0.0	0.077	100	0	0	0.97	0.0	0.003	100	0	0
BC	8.2	0.0	0.013	100	0	0	1.6	0.0	0.002	100	0	0
HD	1.8	0.0	0.010	100	0	0	1.0	0.0	0.006	100	0	0
BCD	0.24	0.0	0.003	100	0	0	0.12	0.0	0.001	100	0	0

Table 5. Estimated diffuse and point contributions to summer (2013 and 2014) P loads, P yields, and the proportion of time that P loads are point source dominated. Values derived from load apportionment modelling

Sub-watershed	2013 Summer						2014 Summer					
	DS load (t)	PS load (t)	DS yield (t/km^2)	DS load as % of annual load	PS load as % of annual load	% time PS load dominant	DS load (t)	PS load (t)	DS yield (t/km^2)	DS load as % of annual load	PS load as % of annual load	% time PS load dominant
TP												
WBLS	1.2	0.47	0.018	62	38	40	2.1	0.47	0.032	76	24	29
EC	1.4	0.0	0.002	100	0	0	8.6	0.0	0.014	100	0	0
TC	4.9	0.0	0.014	100	0	0	0.24	0.0	0.001	100	0	0
DHC	3.1	1.5	0.020	53	47	78	0.74	0.03	0.003	94	4	9
SC	5.0	0.0	0.018	100	0	0	0.17	0.0	0.001	100	0	0
BC	3.1	0.0	0.008	100	0	0	0.67	0.0	0.000	100	0	0
HD	2.1	0.0	0.012	100	0	0	0.18	0.0	0.001	99	1	0
BCD	0.13	0.0	0.002	100	0	0	1.2	0.0	0.015	100	0	0
TDP												
WBLS	0.91	0.26	0.014	71	29	27	1.7	0.30	0.026	83	17	23
EC	0.74	0.0	0.001	100	0	0	6.6	0.0	0.011	100	0	3
TC	1.3	0.0	0.004	100	0	0	0.21	0.0	0.001	100	0	0
DHC	3.9	0.42	0.017	90	10	7	0.50	0.03	0.002	94	6	11
SC	0.76	0.00	0.003	100	0	0	0.064	0.0	0.000	100	0	0
BC	1.9	0.0	0.002	100	0	0	0.47	0.007	0.000	99	1	0
HD	1.4	0.0	0.008	100	0	0	0.14	0.001	0.001	99	1	0
BCD	0.15	0.0	0.002	100	0	0	0.95	0.0	0.011	100	0	0
SRP												
WBLS	0.43	0.19	0.010	60	40	75	1.6	0.33	0.028	80	20	34

	EC	0.34	0.0	0.001	100	0	0	4.3	0.0	0.007	100	0	0
	TC	1.1	0.0	0.003	100	0	0	0.46	0.0	0.001	100	0	0
	DHC	3.1	0.94	0.018	70	30	62	0.44	0.10	0.002	78	22	47
	SC	0.65	0.0	0.002	100	0	0	0.064	0.0	0.000	100	0	0
	BC	1.6	0.0	0.002	100	0	0	0.47	0.0	0.001	100	0	0
	HD	0.51	0.0	0.003	100	0	0	0.11	0.0	0.001	100	0	0
	BCD	0.11	0.0	0.002	100	0	0	0.85	0.0	0.010	100	0	0
PP													
	WBLS	0.48	0.0	0.007	100	0	0	0.36	0.0	0.006	100	0	0
	EC	1.0	0.0	0.002	100	0	0	3.6	0.0	0.006	100	0	0
	TC	3.7	0.0	0.011	100	0	0	0.14	0.001	0.000	100	0	0
	DHC	3.0	0.12	0.014	91	9	11	0.22	0.001	0.001	100	0	0
	SC	1.4	0.0	0.005	100	0	0	0.054	0.00	0.000	100	0	0
	BC	1.0	0.0	0.006	100	0	0	1.1	0.0	0.000	100	0	0
	HD	2.7	0.0	0.015	100	0	0	0.04	0.0	0.000	100	0	0
	BCD	0.013	0.0	0.000	100	0	0	0.34	0.0	0.004	100	0	0

Fig. 1 a-d

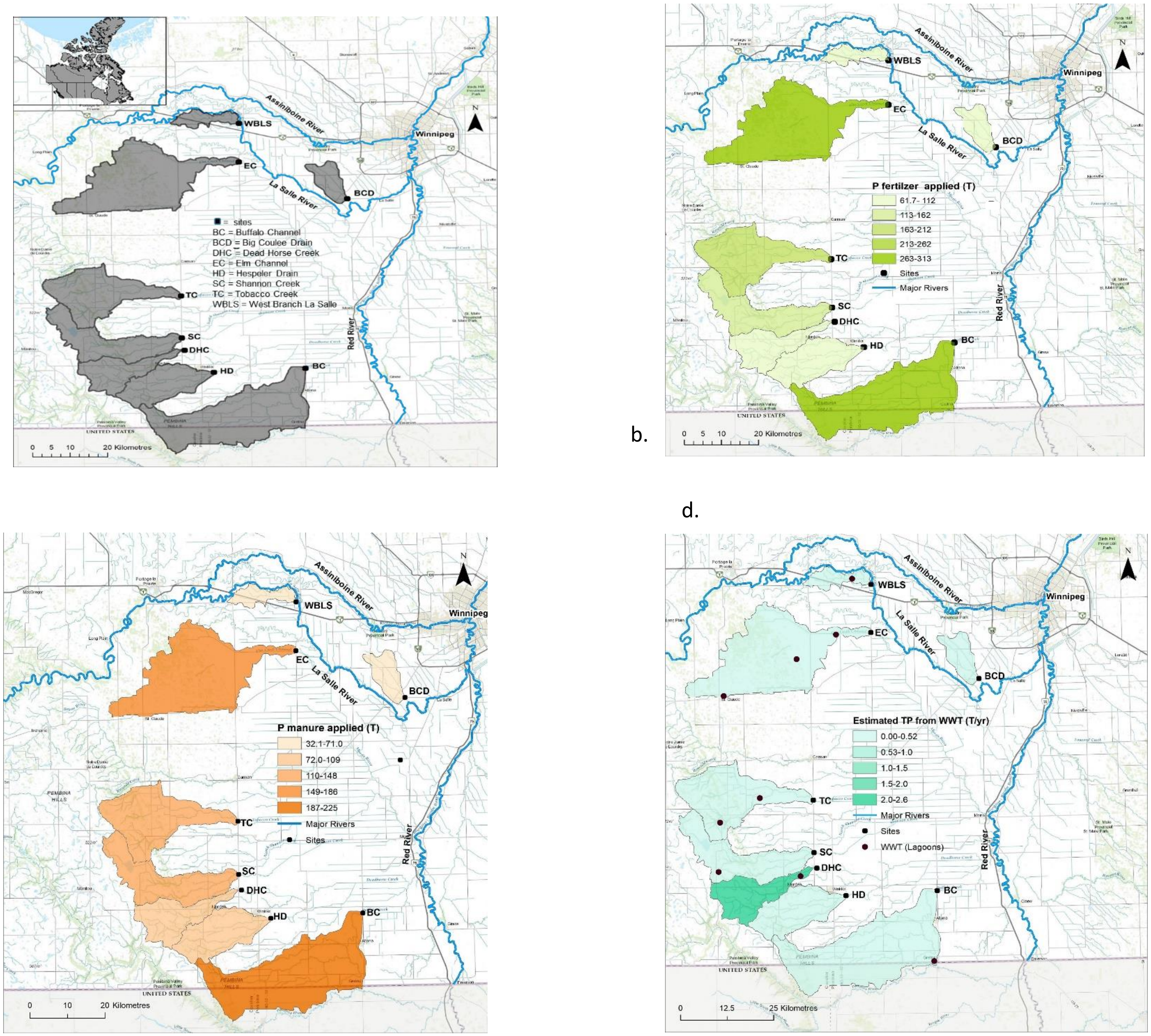
Assiniboine River
Winnipeg
La Salle River
Red River
WBLS
EC
BCD
TC
SC
DHC
HD
BC
= sites
BC = Buffalo Channel
BCD = Big Coulee Drain
DHC = Dead Horse Creek
EC = Elm Channel
HD = Hespeler Drain
SC = Shannon Creek
TC = Tobacco Creek
WBLS = West Branch La Salle
UNITED STATES
0 5 10 20 Kilometres
b.
P fertilzer applied (T)
61.7- 112
113-162
163-212
213-262
263-313
Sites
Major Rivers
P manure applied (T)
32.1-71.0
72.0-109
110-148
149-186
187-225
Major Rivers
Sites
0 10 20 Kilometres
d.
Estimated TP from WWT (T/yr)
0.00-0.52
0.53-1.0
1.0-1.5
1.5-2.0
2.0-2.6
Major Rivers
Sites
WWT (Lagoons)
0 12.5 25 Kilometres

Fig. 2

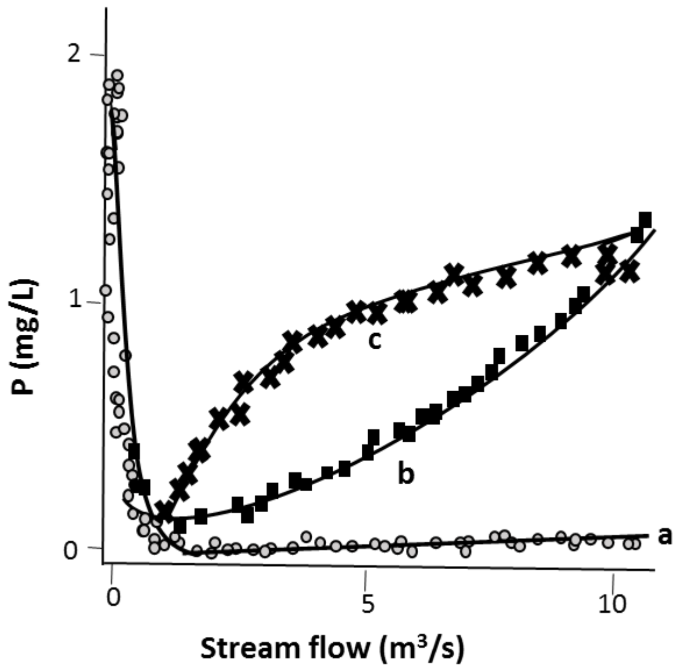

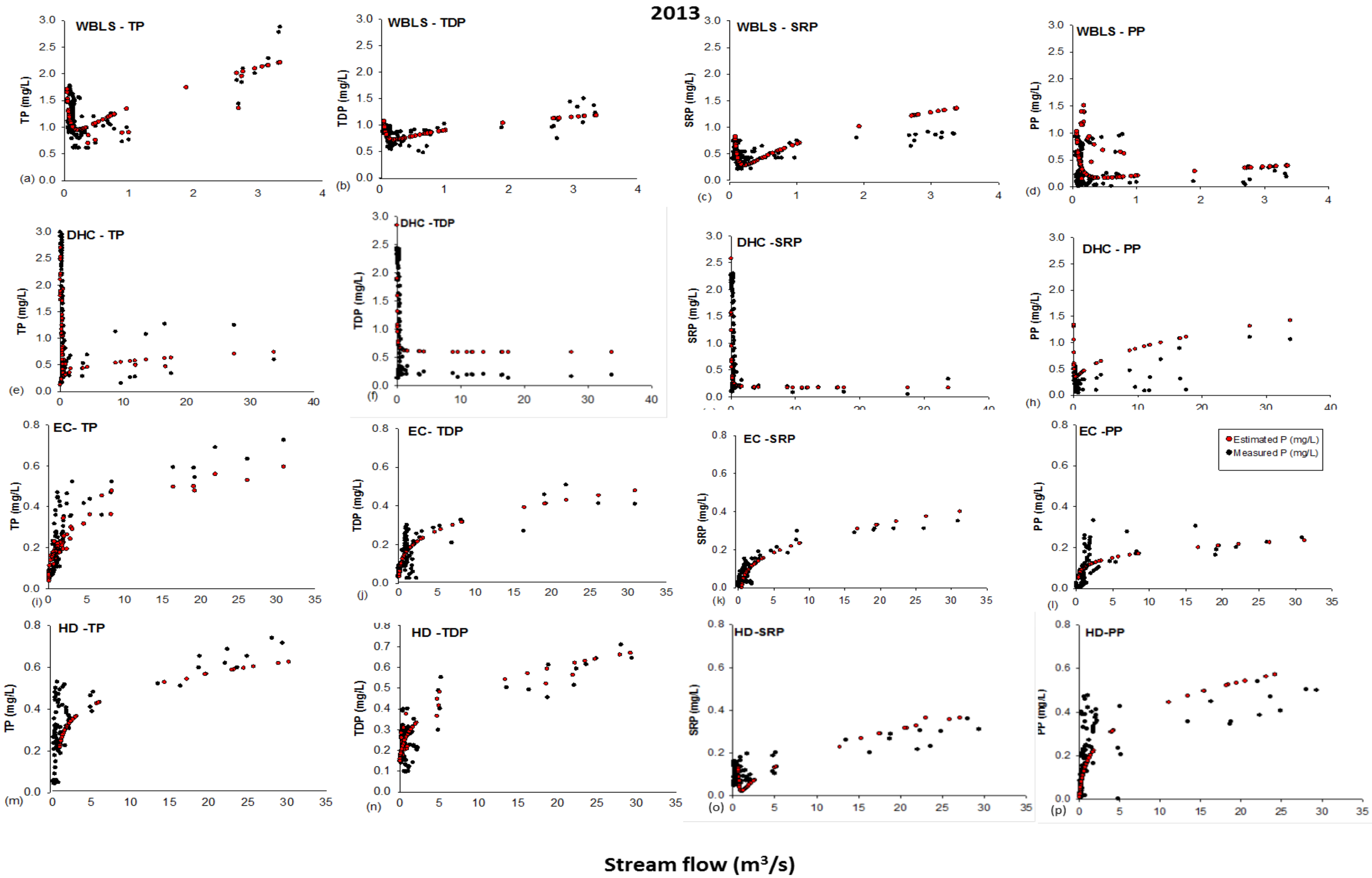
2013
WBLS - TP
WBLS - TDP
WBLS - SRP
WBLS - PP
DHC - TP
DHC -TDP
DHC -SRP
DHC - PP
EC- TP
EC- TDP
EC -SRP
EC -PP
HD -TP
HD -TDP
HD-SRP
HD-PP
TP (mg/L)
TDP (mg/L)
SRP (mg/L)
PP (mg/L)
Estimated P (mg/L)
Measured P (mg/L)
Stream flow (m³/s)

Fig. 3 annual

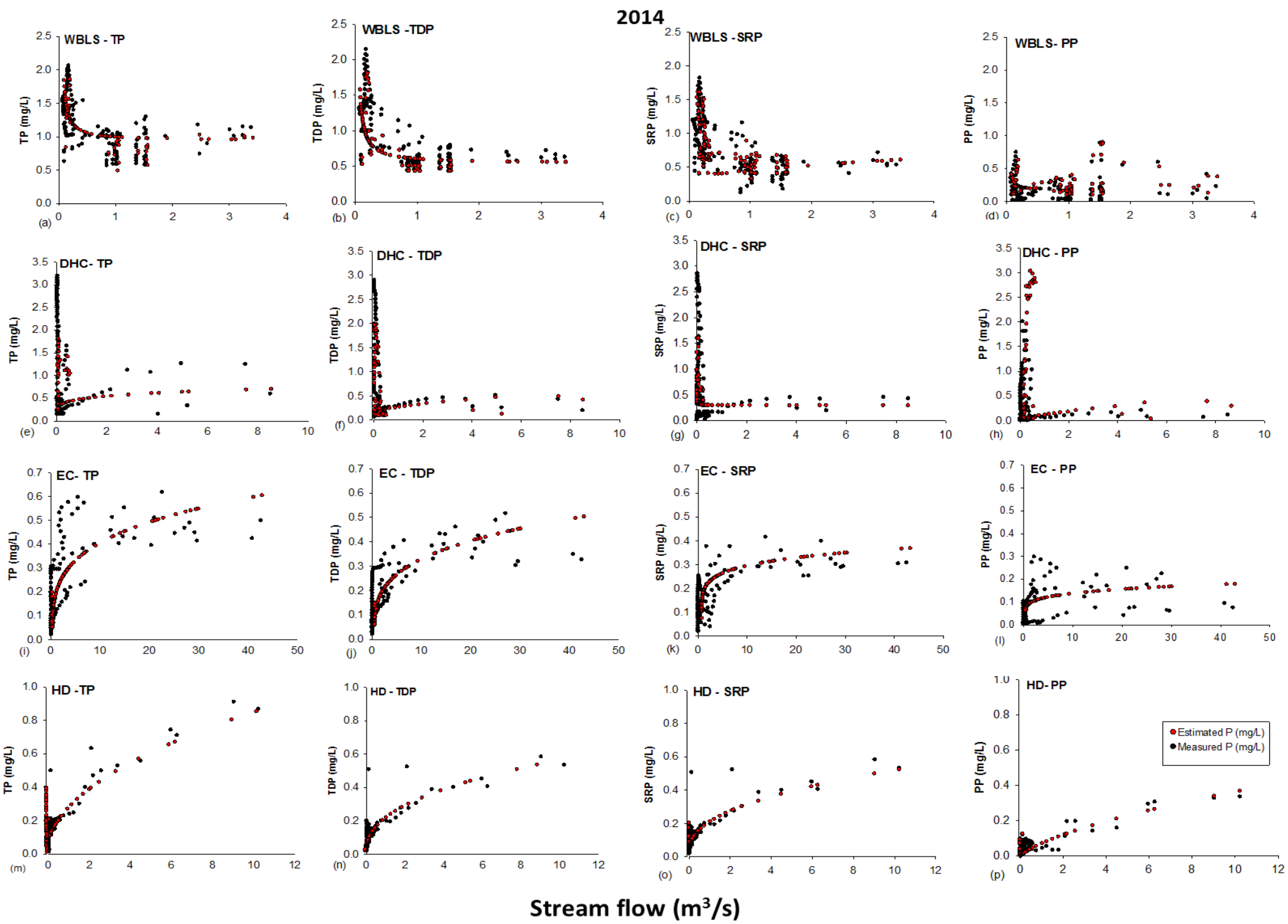

Fig.4 LAM 2014

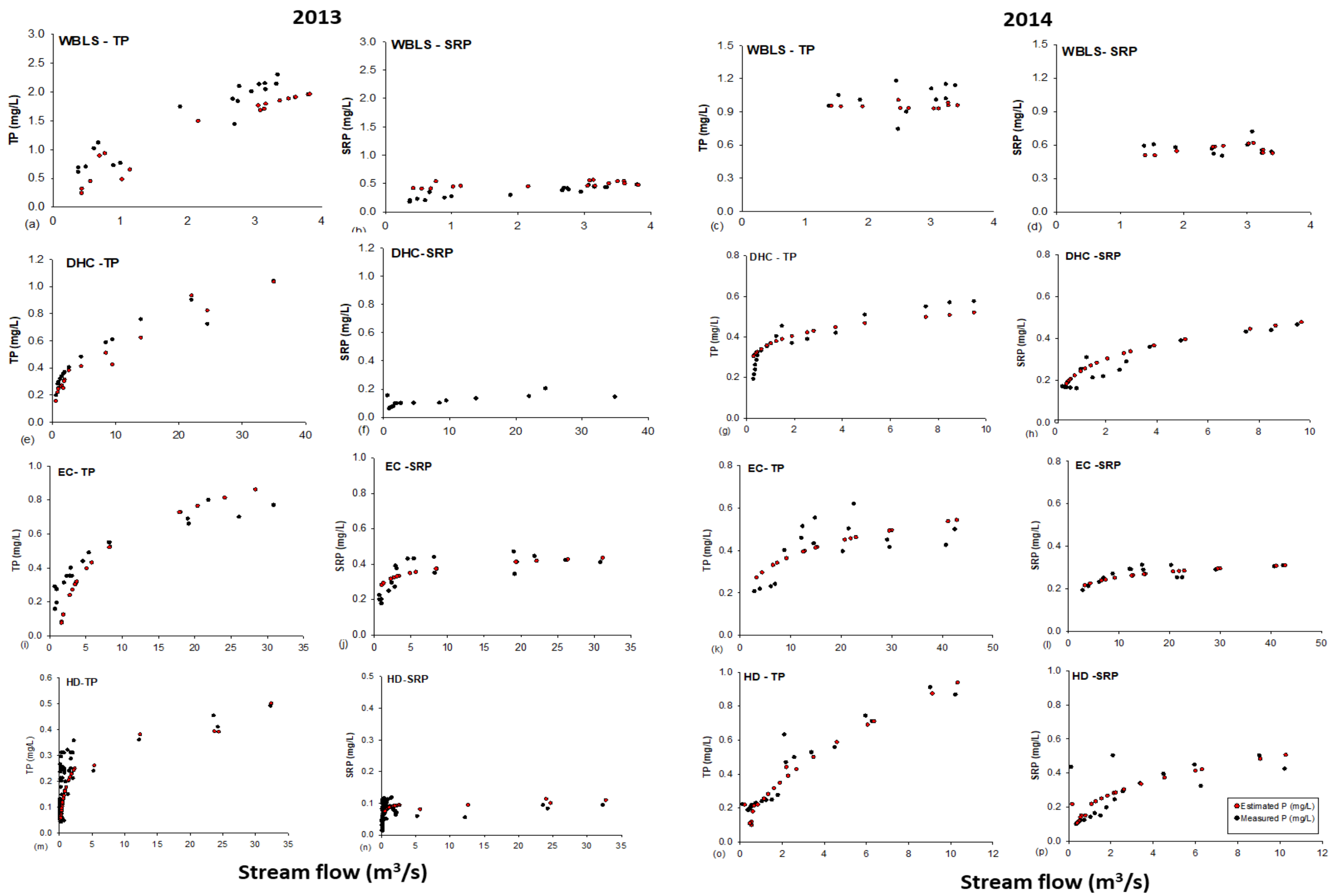

Fig. 5 LAM snowmelt

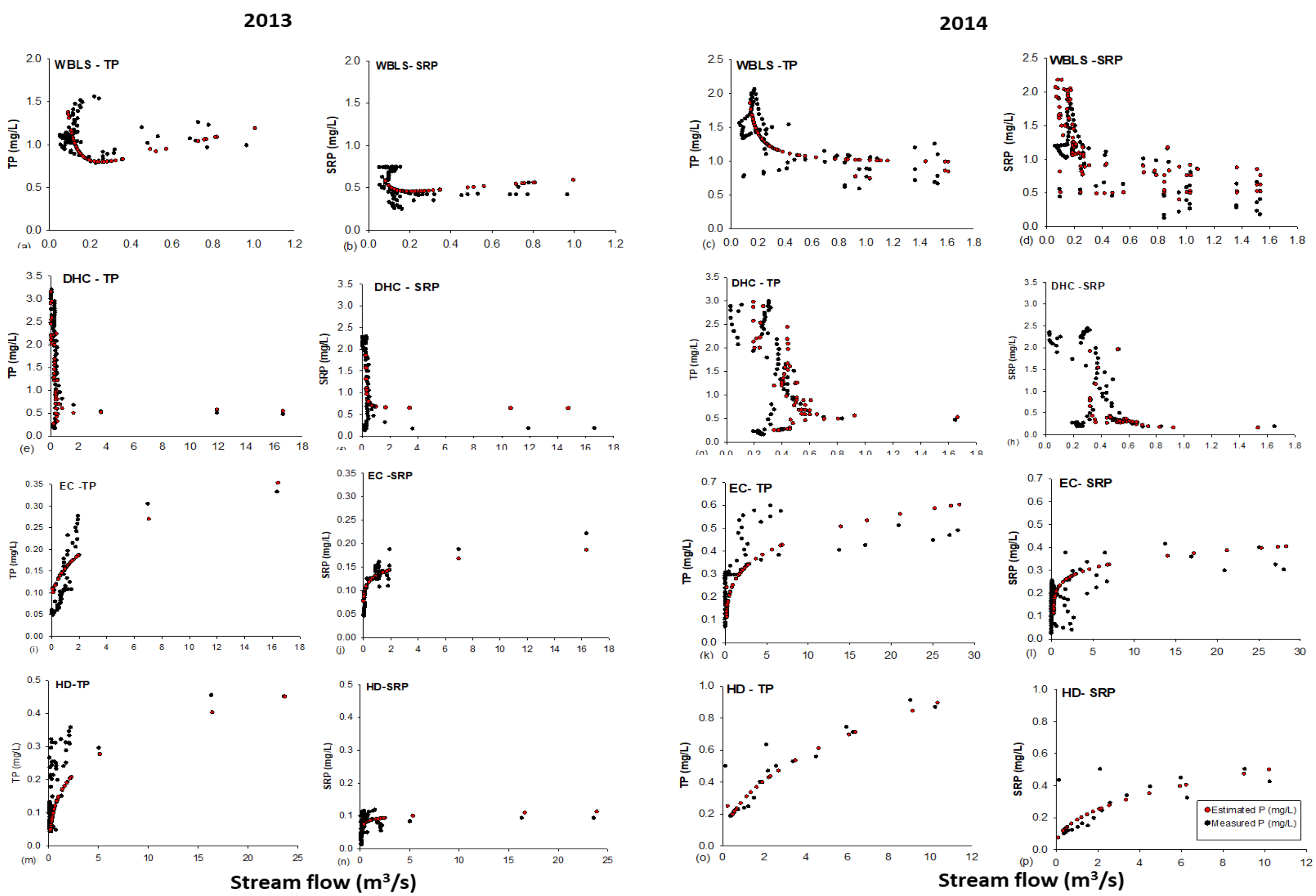

Fig. 6 Summer LAM

1